A Photonic Spectrum Analyzer for Waveguide-Coupled Sources in the Terahertz Range

Benedikt Leander Krause, Amlan kusum Mukherjee, and Sascha Preu, *Member, IEEE*

***Abstract*—Signals in the terahertz range are mainly wireless, waveguide-bound or on-chip signals. To measure their spectral power, linewidth and harmonics, usually spectrum analyzers are used. Here we present a photonic spectrum analyzer for waveguide-bound signals for the frequency range from 450 GHz to 1.05 THz with the possibility to extend its operation to on-chip signals. Therefore, a photonically generated local oscillator frequency is used to downconvert the signal under test within a photoconductor. A Vivaldi antenna feeds the signal from a dielectric waveguide to the photoconductor. This allows the measurement of any signal that can be transported via a dielectric waveguide. We show details on the transition from a rectangular metallic hollow waveguide to a dielectric waveguide and spectral measurements of a rectangular metallic hollow waveguide source. The same transition can also be used to attach metallic waveguide-coupled ground-source-ground probes in order to characterize on-chip sources.**

***Index Terms*—Photomixer, photonic local oscillator, spectrum analyzer, dielectric waveguide, dielectric rod waveguide antenna, waveguide, terahertz spectrum.**

I. Introduction

With rising interest in applications at Terahertz (THz) frequencies, reliable, versatile and affordable THz measurement equipment becomes more and more important. To date, frequency-extended microwave electronic measurement equipment, like spectrum analyzers (SAs) or vector network analyzers (VNAs), dominates the market. Extender modules are usually connected with metallic hollow waveguides (MHWGs) [1] limited to single-mode operation with a bandwidth of at best 50% of the center frequency. In order to cover a larger spectrum, e.g. from 100 GHz to 1 THz at least six extender modules are needed [2], [3]. Each band must be individually aligned and calibrated. The higher the THz frequency, the (exponentially) more expensive the extender will be.

With a photonically generated local oscillator (LO) and a photoconductive antenna (PCA) employed as a mixer, we have shown that a single setup is able to measure the full range from below 100 GHz to 1 THz at the example of a free-space photonic spectrum analyzer (PSA) [4] and a free-space photonic vector network analyzer [5]. The LO was generated by the difference frequency of two frequency-adjustable continuous-wave, distributed feedback laser diodes. So far, the photonic setup employed logarithmic-periodic antennas and a silicon lens, limiting measurements to free-space coupled sources under test. Many THz sources, in particular electronic ones, are frequently on-chip or mounted in a MHWG [6], [7] therefore requiring on-chip or in-waveguide measurement capabilities. In this paper, we demonstrate a PSA using a planar PCA, enabling the measurement of waveguide-bound signals. We verify this by the exemplary characterization of a WR2.2-coupled VNA head. For this we discuss the transition from the photonic circuit to a MHWG in detail. The very same transition can also be employed for characterization of on-chip sources via MHWG-coupled, commercially available ground-signal-ground (GSG) cascade probes.

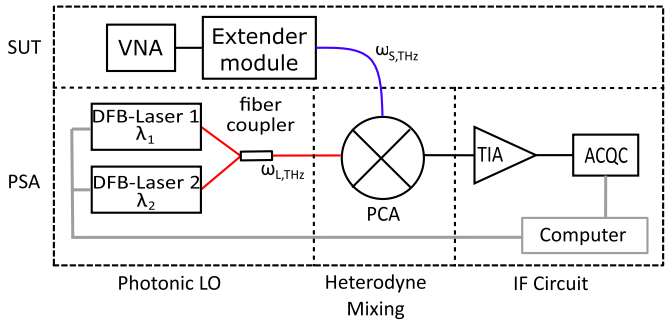

Fig. 1. Schematic of the photonic spectrum analyzer with the SUT.

II. Measurement-Setup

A. Photonic Spectrum Analyzer

The PSA consists of two frequency-adjustable distributed feedback (DFB) laser diodes, a PCA, a trans-impedance amplifier (TIA) and an acquisition card (ACQC) as illustrated in Fig. 1. The PSA mixes the signal under test (SUT) with the beat signal of the two lasers within the PCA [4]. This results in an intermediate frequency signal whose spectral power at or around the laser beat frequency is obtained after filtering and squaring. Sweeping the beat signal frequency and simultaneously measuring the IF signal creates a frequency spectrum of the SUT. The difference to the PSA version in [4] is the PCA. The logarithmic-periodic antenna and the silicon lens are replaced by a broadband planar end-fire Vivaldi antenna (VA) [8], similar to the one shown in [9],

Manuscript received 29 July 2022; revised 22 November 2022; accepted 25 January 2023. Date of publication 31 January 2023; date of current version 15 February 2023. This work was supported in part by European Research Council (ERC) "Pho-T-Lyze", under Grant 713780 and in part by the ERC Proof-of-Concept "PhoSTer THz", under Grant 101057162. *(Corresponding author: Benedikt Leander Krause.)*

The authors are with the Department of Electrical Engineering and Information Technology, Technical University of Darmstadt, 64283 Darmstadt, Germany (e-mail: benedikt.krause@tu-darmstadt.de; amlan.mukherjee@tu-darmstadt.de; sascha.preu@tu-darmstadt.de).

Color versions of one or more figures in this article are available at https://doi.org/10.1109/JSTQE.2023.3241017.

Digital Object Identifier 10.1109/JSTQE.2023.3241017

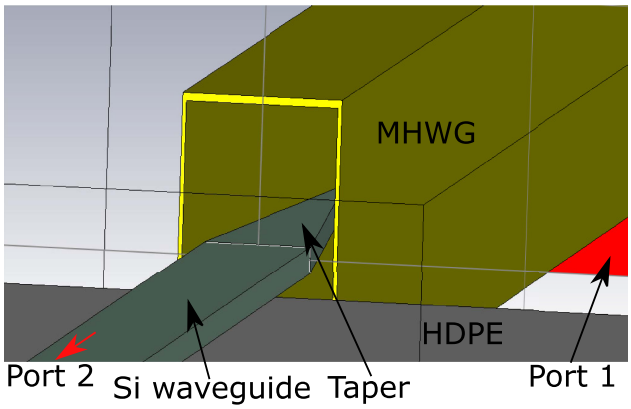

Fig. 2. Simulation profile of the WR2.2 MHWG to Si waveguide transition.

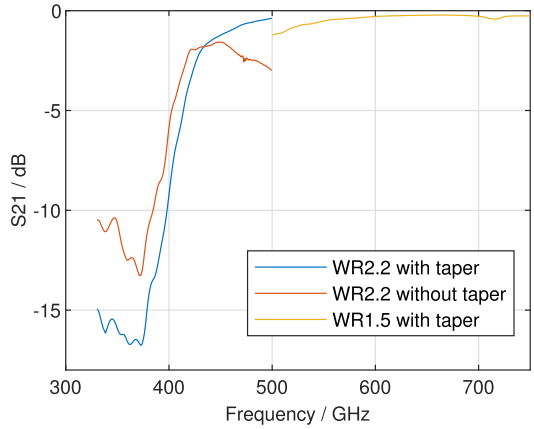

Fig. 3. Simulated transmission of different MHWG to Si waveguide transitions.

coupled to a dielectric waveguide [9], [10]. Both are designed to enable planar PSAs and photonic VNAs and operate between 450 GHz and 1.05 THz [9], [10], [11]. The dielectric waveguide is a planar rectangular waveguide consisting of highly resistive float zone silicon as this offers a low loss material with a high refractive index and a good surface roughness control. The implemented Si waveguides have a size of 200 μm $\times$ 50 μm, an attenuation of 0.1 dB/cm and support bending radii down to 2 mm [9].

B. Dielectric to Metallic Hollow Waveguide Transition

Generalov et al. [12] demonstrated a low loss tapered dielectric rod waveguide antenna transition coupling to the TE_{10} mode typically used in MHWGs. The TE_{10} mode within the MHWG couples into the HE_{11} mode within the dielectric rod waveguide antenna, i.e. the fundamental mode of the dielectric waveguide [13]. In order to estimate the coupling losses, the transition from a WR2.2 MHWG to a highly resistive float zone silicon (Si) waveguide using a taper length of 1 mm is simulated with CST microwave studio. Fig. 2 shows the setup where the full length of the taper is put inside the MHWG. The Si waveguide is placed partially onto a high density polyethylene (HDPE) carrier in order to mechanically stabilize the waveguide. The simulations are done only taking the aforementioned fundamental modes into account. Three different scenarios are simulated. First the transition from a WR2.2 MHWG to a Si waveguide with the aforementioned taper fully inside the WR2.2 waveguide. This is done for the supported frequencies of the WR2.2 waveguide, namely between 330 GHz and 500 GHz. Secondly, the same transition using a Si waveguide without taper, having the Si waveguide inserted 1 mm into the WR2.2 waveguide. As tapers get smaller towards their tips, it is possible to also use them for higher frequency MHWGs [14]. Therefore, thirdly, the transition from a WR1.5 MHWG (supported frequencies 500 GHz to 750 GHz) to a Si waveguide using the same taper is simulated. Since this MHWG features an inner cross section of 380 μm $\times$ 190 μm the taper is only inserted by 0.8 mm.

The VA, due to its physical size, in conjunction with the Si waveguide have a lower cut-off frequency of approximately 450 GHz [9] while the WR2.2 MHWG is used starting from 330 GHz. As frequencies below 450 GHz will not be detected efficiently, they are not discussed further. For the frequency range from 450 GHz to 500 GHz the simulation indicates transmission from the MHWG to the Si waveguide with taper being better than -1.3 dB Fig. 3. For the frequency range of the WR1.5 MHWG the simulated results also show better than -1.3 dB transmission. For the WR2.2 MHWG transition without taper the results drop down to values between -3 dB and -1.6 dB for the frequencies above 450 GHz. As the difference between the simulations with and without taper for the WR2.2 MHWG are minor, the simpler and easier to manufacture version without any taper will be used throughout this paper.

III. Results

Fig. 1 depicts the SUT, namely a vector network analyzer (VNA; Keysight PNA) with a WR2.2 extender module (Virginia Diodes VNAX WM-570 (WR2.2)) [3] with a frequency coverage from 330 GHz to 500 GHz. The VNA frequency was kept constant and the power was set to the maximum power allowed for the extender module of 10 dBm resulting in an output power in the WR2.2 band between -5 dBm and 0 dBm [3]. For the PSA two telecom DFB lasers, controlled by a TeraScan DLC smart (Toptica Photonics), provide a difference frequency, corresponding to the LO frequency, between 0 GHz and 1250 GHz. The LO frequency is adjustable in 1 MHz steps and features a ms-scale linewidth and stability of about 1.2 MHz. A Femto DHPCA-100 TIA in the post detection circuit provides a transimpedance gain of 10^7 V/A. The ACQC is an Advantech PCIE-1840 L, set to an acquisition rate of 5 MSa/s and an acquisition range of ± 0.1 V. The intermediate frequency range is limited by the TIA to 220 kHz. The PCA consists of an ErAs:In(Al)GaAs photomixer with a Vivaldi antenna on an InP-substrate [8]. The Vivaldi antenna is connected to a Si waveguide with the dimensions of 200 μm $\times$ 50 μm. The Si waveguide features a 90° bend and a total length of approximately 4 cm Fig. 4. The untapered Si waveguide is partially inserted into the center of the MHWG.

In a first measurement the Si waveguide is inserted by approximately 1 mm into the MHWG in agreement with the simulation. The VNA with extender frequency is set to 480 GHz.

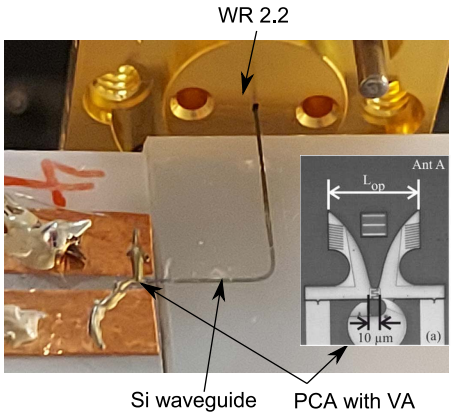

Fig. 4. Transition between the metallic and the Si waveguide with a closeup on the PCA (©IEEE (2021) reused with permission from [14]).

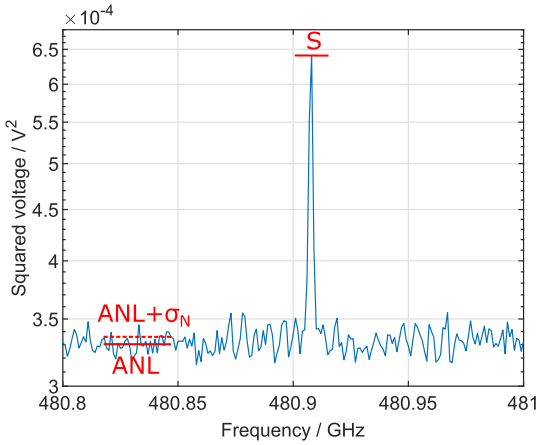

Fig. 5. Measured signal at 480 GHz.

Fig. 5 shows the spectrum of the SUT at 480 GHz taken with the PSA with frequency steps of 1 MHz from 480.8 GHz to 481 GHz with an averaging time of 200 ms per point. The signal is clearly visible at a frequency of 480.9 GHz instead of the expected 480 GHz, pointing to a miscalibration of the frequency of possibly both the PSA LO and the VNA with a total offset of 900 MHz. By recalibrating the look-up tables of the LO, we expect the offset to become less than 25 MHz. Please note that the Y-axis is given in units of V^2, which is directly proportional to power. Unfortunately, no power calibration could be conducted as none of our available power meter allow for reliable power measurements within the WR2.2 MHWG. Previously [4], we determined the displayed average noise power of the PSA to be $-100\,\mathrm{dB/Hz}$ at 500 GHz.

The signal shows an average noise level (ANL) that is more than ten times larger than the noise standard deviation σ_N. The ANL consists not only of a noise offset that is generated from squaring the signal but also of any remaining offset from the IF circuit. The exact reasons for these offsets are not known to date but their removal will be part of future work. Nonetheless, σ_N limits securely identifying the signal under test. To achieve this consistently, and even if standing waves are present, the limit of detection is set to five times σ_N above the average noise level (ANL): $ANL + 5\,\sigma_N$. In order to compare the results from

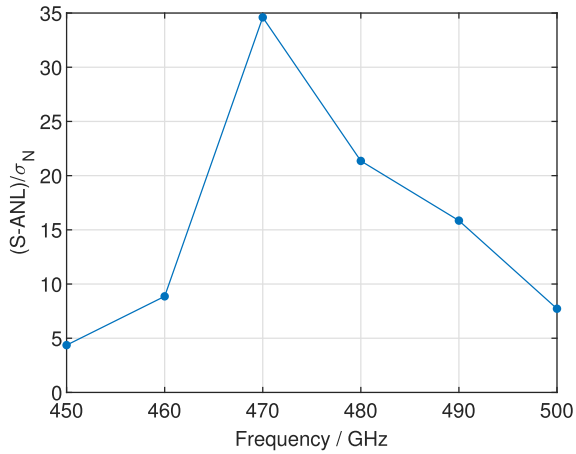

Fig. 6. Signal to noise standard deviation ratio at frequencies between 450 GHz and 500 GHz.

different measurements, each signal is normalized to their corresponding σ_N as $(S - ANL)/\sigma_N$. S is the respective maximum of each signal.

In order to examine the frequency response of the SUT and PSA combination, the frequency in the extender is set to 500 GHz and decreased by 10 GHz after each measurement until the SUT is below the limit of detection. For each of the measurements the frequency range of the PSA is set to match the SUT while keeping all of the other settings the same. Fig. 6 displays the detectability of the signal at different frequencies. The measured results show the highest detectability at a frequency of 470 GHz. Signals at and below 450 GHz are below the limit of detection while frequencies above 500 GHz are not supported by the SUT. The results shown in Fig. 6 are a combined outcome of the SUT power, the transition from the MHWG to the Si waveguide, the transition to the PCA and the responsivity of the PCA. Therefore, it is not possible to directly compare the measured results with the simulation results Fig. 3.

In order to determine the optimum insertion depth of the Si waveguide into the WR2.2 MHWG, the Si waveguide is first positioned 2.1 mm inside the waveguide and then pulled out in 200 μm steps. At each of the positions a spectrum of the SUT is taken, using the same settings and the same VNA frequency as the first measurement. In Fig. 7 the position Zero marks where the end facet of the silicon waveguide is in the plane of the MHWG port. Negative positions refer to increasing the distance between the Si waveguide end facet and the MHWG and positive values mean that it is moved inside the MHWG. The position Zero was visually determined with a microscope resulting in an error bar of 100 μm. The red line marks the limit of detection of $5\,\sigma$. This limit allows to still securely identify the signal, even when standing waves are present.

The $5\,\sigma$ level is just reached at Zero. The further the Si-waveguide is inserted into the MHWG, the larger the $(S - ANL)/\sigma_N$ gets, with a maximum at 1.7 mm.

IV. Conclusion

We have demonstrated a photonic spectrum analyzer with a low-loss interface to metallic hollow waveguides. The transition

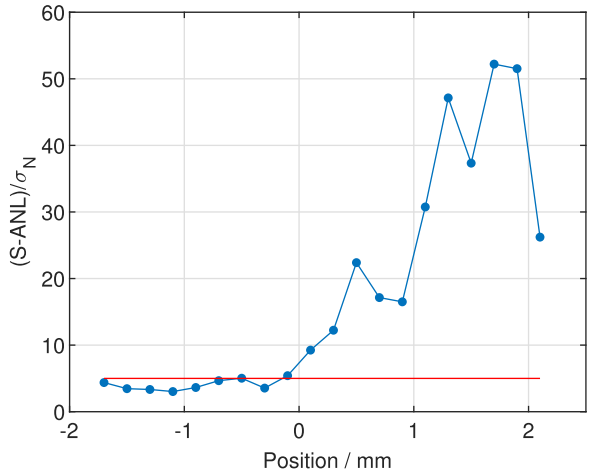

Fig. 7. Signal to noise standard deviation ratio at different positions. Position = 0 mm marks the point, at which the Si-waveguide leaves the metallic one. The red line is the detection limit at $5\,\sigma$.

is based on a rectangular, dielectric silicon waveguide connected to a Vivaldi-antenna with an ErAs:InGaAs photoconductor as mixer. The WR2.2 transition can be realized as a tapered dielectric rod waveguide or by a terminated straight end facet. The transition can serve to investigate WR-coupled devices by the photonic spectrum analyzer or to serve as an on-chip transition by using a WR-coupled GSG probe being the conventional means to interface circuits. Further applications are implementations in photonic vector network analyzers where they would serve as an interface to WR-coupled devices under test. If some losses are acceptable, the same dielectric waveguide can be used for several metallic hollow waveguide bands as demonstrated already in [15].

REFERENCES

[1] R. Sorrentino and G. Bianchi, *Microwave and RF Engineering*, 1st ed. Chichester, U.K.: Wiley, 2010.
[2] T. Ozturk, O. Morikawa, I. Ünal, and I. Uluer, "Comparison of free space measurement using a vector network analyzer and low-cost-type THz-TDS measurement methods between 75 and 325 GHz," *J. Infrared Milli Terahz Waves*, vol. 38, pp. 1241–1251, 2017.
[3] Virginia Diodes Inc., "Vector Network Analyzer Extenders," Accessed: Jun. 10, 2022. [Online]. Available: https://www.vadiodes.com/en/products/vector-network-analyzer-extension-modules
[4] B. L. Krause, A. d. J. Fernandez Olvera, and S. Preu, "Photonic spectrum analyzer for wireless signals in the THz range," *IEEE Access*, vol. 10, pp. 42047–42054, 2022.
[5] A. D. J. F. Olvera, A. K. Mukherjee, and S. Preu, "A fully optoelectronic continuous-wave 2-port vector network analyzer operating from 0.1 THz to 1 THz," *IEEE J. Microw.*, vol. 1, no. 4, pp. 1015–1022, Oct. 2021.
[6] S. Gong et al., "Terahertz meta-chip switch based on C-ring coupling," *Nanophotonics*, vol. 11, no. 9, pp. 2037–2044, 2022.
[7] H. Zhu et al., "Terahertz on-chip tunable spoof surface plasmon polaritons transmission lines based on vanadium oxide," in *Proc. IEEE MTT-S Int. Microw. Workshop Ser. Adv. Mater. Process. RF THz Appl.*, Chongqing, China, 2021, pp. 100–102.
[8] M. F. Abdullah, A. K. Mukherjee, R. Kumar, and S. Preu, "Vivaldi end-fire antenna for THz photomixers," *Int. J. Infrared Millim. Waves*, vol. 41, pp. 728–739, 2020.
[9] A. K. Mukherjee, M. Xiang, and S. Preu, "Broadband terahertz photonic integrated circuit with integrated active photonic devices," *MDPI Photon.*, vol. 8, no. 11, 2021, Art. no. 492.
[10] A. K. Mukherjee, M. Xiang, and S. Preu, "Broadband Dielectric Waveguides for 0.5–1.1 THz Operation," in *Proc. IEEE 45th Int. Conf. Infrared, Millimeter, Terahertz Waves*, Buffalo, NY, USA, 2020, pp. 1–2.
[11] A. J. Marcatili, "Dielectric rectangular waveguide and directional coupler for integrated optics," *Bell Syst. Tech. J.*, vol. 48, no. 7, pp. 2071–2102, 1969.
[12] A. A. Generalov, J. A. Haimakainen, D. V. Lioubtchenko, and A. V. Räisänen, "Wide band mm- and sub-mm-wave dielectric rod waveguide antenna," *IEEE Trans Terahertz Sci Technol*, vol. 4, no. 5, pp. 568–574, Sep. 2014.
[13] H.-T. Zhu et al., "Low-loss, thermally insulating, and flexible rectangular dielectric waveguide for Sub-THz-Signal coupling in superconducting receivers," *IEEE Trans. Terahertz Sci. Technol.*, vol. 10, no. 2, pp. 190–199, Mar. 2020.
[14] A.k. Mukherjee, M. Xiang, and S. Preu, "Antenna designs for near field waveguide coupling between 0.6 and 0.9 THz," in *Proc. 46th Int. Conf. Infrared, Millimeter Terahertz Waves*, Chengdu, China, 2021, pp. 1–2.
[15] A. A. Generalov, D. V. Lioubtchenko, and A. V. Räisänen, "Dielectric Rod Waveguide Antenna at 75–1100 GHz," in *Proc. IEEE 7th Eur. Conf. Antennas Propag.*, Gothenburg, Sweden, 2013, pp. 541–544.

Benedikt Leander Krause received the B.Sc. degree in electronic and sensor materials from Technical University Bergakademie Freiberg, Freiberg, Germany, in 2015, and the M.Sc. degree in electrical engineering from Friedrich-Alexander University Erlangen-Nürnberg, Erlangen, Germany, in 2019. He is currently working toward the Ph.D. degree with the Technical University of Darmstadt, Darmstadt, Germany. In 2020, he joined the Terahertz Devices and Systems Laboratory with the Technical University of Darmstadt. His research interests include the development of photonic spectrum analyzers using photoconductive mixers for the terahertz range.

Amlan kusum Mukherjee received the B.Tech. degree in electronics and communication engineering from the National Institute of Technology, Durgapur, India, in 2013, and the M.Sc. degree in information and communication engineering from the Technical University (TU) of Darmstadt, Darmstadt, Germany, in 2018. Since 2018, he has been working toward the Ph.D. degree with the Terahertz Devices and Systems Group, TU Darmstadt. His research interests include terahertz imaging, dielectric waveguides, and photonic integrated circuits for terahertz operation.

Sascha Preu (Member, IEEE) received the Diploma and Ph.D. degrees (*summa cum laude*) in physics from the University of Erlangen-Nuremberg, Erlangen, Germany, in 2005 and 2009, respectively. From 2004 to 2010, he was with the Max Planck Institute for the Science of Light, Erlangen, Germany. From 2010 to 2011, he was with Materials and Physics Department, University of California at Santa Barbara, Santa Barbara, CA, USA, in the framework of a Feodor Lynen stipend by the Humboldt foundation. From 2011 to 2014, he was with the Chair of Applied Physics, University of Erlangen-Nuremberg. He is currently Full Professor with the Department of Electical Engineering and Information Technology, Technical University of Darmstadt, Darmstadt, Germany, leading the Terahertz Devices and Systems laboratory. His research interests include the development of semiconductor-based terahertz sources and detectors, including photomixers, photoconductors, and field-effect transistor rectifiers, spintronic devices, development of powerful terahertz systems as well as applications of terahertz radiation. In 2017, he was the recipient of the ERC starting Grant for developing ultrabroadband, photonic terahertz signal analyzers and in 2022 a Proof of Concept Grant on development of photonic spectrum analyzers towards commercial exploitation.